Pharmaceutical Research, Vol. 23, No. 10, October 2006 (© 2006)
DOI: 10.1007/s11095-006-9022-5

Research Paper

Investigation of the Multi-Step Dehydration Reaction of Theophylline Monohydrate Using 2-Dimensional Powder X-ray Diffractometry

Cletus Nunes,[1,2] Arumugam Mahendrasingam,[3] and Raj Suryanarayanan[1,4]

Received January 16, 2006; accepted March 29, 2006; published online September 1, 2006

Purpose. (i) To study the dehydration kinetics of theophylline monohydrate using 2-dimensional (2D) powder X-ray diffractometry (XRD), and (ii) to investigate the effect of polyvinylpyrrolidone (PVP) on the dehydration pathway and kinetics.
Methods. Theophylline monohydrate ($C_7H_8N_4O_2{\cdot}H_2O$; **M**) was recrystallized from aqueous PVP solutions of different concentrations. Dehydration kinetics was studied isothermally, at several temperatures, from 35 to 130°C. The experimental set-up comprised of a high intensity X-ray source (synchrotron radiation or 8 kW rotating anode), a heating chamber, and a 2D area detector. Diffraction patterns were collected continuously, with a time resolution ranging from 40 ms to 30 s, over the angular range of 3 to 27°2θ.
Results. Dehydration of **M** resulted in either the stable ($C_7H_8N_4O_2$; **A**), or the metastable anhydrate (**A***), with the latter having a tendency to transform to **A**. The XRD technique allowed simultaneous quantification of **M**, **A*** and **A** during the dehydration reaction. The rate constants for individual reaction steps (**M**→**A***; **M**→**A** and **A***→**A**) were determined by fitting the data to solid-state reaction models. In presence of PVP, there was a decrease in the magnitude of the rate constant associated with the **M**→**A** transition, resulting in an increased build-up of **A*** in the product. The inhibitory effect of PVP on **M**→**A** transition was more pronounced at lower dehydration temperatures, and was proportional to the concentration of PVP.
Conclusions. Two dimensional powder X-ray diffractometry, using a high intensity source, is a powerful technique to study kinetics of rapid solid-state reactions. The inhibitory effect of excipients can have profound effect on phases formed during pharmaceutical processing.

KEY WORDS: anhydrate; dehydration; metastable; polymorph; synchrotron; theophylline monohydrate; two-dimensional; X-ray diffraction.

INTRODUCTION

Theophylline (3,7-dihydro-1,3-dimethyl-1H-purine-2,6-dione) is a methyl xanthine used in the treatment of bronchial asthma. Theophylline exists either as an anhydrate ($C_7H_8N_4O_2$; **A**) or as a monohydrate ($C_7H_8N_4O_2{\cdot}H_2O$; **M**). The anhydrate and the monohydrate belong to the orthorhombic and the monoclinic crystal systems, respectively (1–3). Both these forms have been the subject of several physical characterization studies (4–11).

When placed in contact with water at ambient temperature, anhydrous theophylline (**A**) rapidly transforms to form **M**. Dehydration of **M** yields back the crystalline anhydrate. Phadnis and Suryanarayanan have reported the formation of a metastable anhydrate (**A***) under certain dehydration conditions (12). It is noteworthy that **A*** was formed only via dehydration of **M** (12,13). The presence of **A*** in the drug product can have serious consequences on product performance. In tablet formulations containing **A***, *in situ* conversion of the **A***→**A** led to an increase in tablet hardness and the tablets failed the USP dissolution test on storage (12).

As seen in the case with theophylline, the solid-state of the active pharmaceutical ingredient (API) in a dosage form should be controlled for ensuring desired product performance during shelf life. This issue is of concern both from a regulatory and intellectual property perspective (14,15). The manufacture of a dosage form entails several unit operations. The API can undergo solid-state transformations during these processes. Consider a general case in which a crystalline anhydrous form of a compound is used as the starting material for tablet manufacture. During aqueous wet granulation, the anhydrate can incorporate water into the lattice and transform to a hydrate. When the granules are dried, the hydrate may yield a metastable phase. This could be a metastable polymorph, as was seen in theophylline, or an incompletely crystalline anhydrate. Thus, even if the starting material is a well-characterized, highly crystalline stable phase, subsequent pharmaceutical processing may cause

[1] Department of Pharmaceutics, University of Minnesota, Minneapolis, Minnesota 55455, USA.
[2] Pharmaceutics R&D, Bristol Myers Squibb Company, New Brunswick, New Jersey 08903, USA.
[3] Department of Physics, Keele University, Staffordshire, ST5-5BG, UK.
[4] To whom correspondence should be addressed. (e-mail: surya001@umn.edu)

build-up of a metastable phase in the final dosage form (16). A mechanistic understanding of phase transitions that occur *during* processing can enable the development of a robust dosage form with reproducible and predictable properties (14,16,17). However, solid state reactions often occur rapidly and involve complex reaction pathways (18,19). In such cases, conventional thermoanalytical techniques (such as differential scanning calorimetry and thermogravimetry) yield complex profiles showing overlapping thermal events (20,21). The concentrations of the individual solid phases *during* the reaction cannot be determined. Thus, the kinetics of the individual reaction steps cannot be studied, and it is difficult to obtain a mechanistic understanding of the reaction pathway/mechanism.

XRD is a powerful technique for solid-state characterization because it can provide direct information on the changes occurring in the crystal lattice of the material (22,23). The dehydration kinetics of **M** has been the subject of several investigations (4,9,11,24). However, the results are in poor agreement and have implicitly assumed a simple **M**→**A** transition. In a recent investigation, Karjalainen *et al*. (2005) have demonstrated the utility of variable temperature XRD to simultaneously monitor the relative amounts of **M**, **A*** and **A** in theophylline granules (25). The effect of two drying methods, on the physical form of theophylline in dried granules was also investigated (Airaksinen *et al*., 2004) (26). However, detailed kinetic studies were not conducted. The dehydration process has also been followed by isothermal microcalorimetry at 40 and 47°C by Duddu *et al*. (10). Interestingly, the authors have proposed that the water loss at 40°C is probably a two-step process. However, the possible formation of the metastable anhydrate (**A***), was not investigated. In light of the above observations, and considering the potential implications of **A*** on a formulation, a thorough investigation of the reaction pathway and kinetics becomes crucial.

Our first objective was to extend the utility of high intensity XRD to obtain a mechanistic understanding of such complex solid-state transitions. Theophylline monohydrate (**M**) was used as the model compound. Using 2-dimensional XRD, the reactant (**M**), intermediate (**A***) and the product (**A**) phases existing during a solid-state reaction were simultaneously quantified. Our second objective was to investigate the effect of an excipient, polyvinylpyrrolidone (PVP), on the dehydration reaction kinetics and pathway. PVP is a commonly used granulating agent during tablet manufacture. PVP is a crystallization inhibitor, and is known to stabilize the metastable anhydrate (**A***) formed on dehydration of **M** (27). Moreover, the inhibitory effect of PVP is influenced by its concentration and molecular weight (27,28). Therefore, our specific interest was to evaluate the effect of PVP on the kinetics of formation of the stable anhydrate (**A**) during dehydration of **M** and to examine the possible build-up of the metastable anhydrous polymorph (**A***) as a dehydrated product.

EXPERIMENTAL

Materials

Anhydrous theophylline was used as received (Sigma Chemical Company, St. Louis, MO).

Preparation of Theophylline Monohydrate

Anhydrous theophylline was dissolved in distilled water at 60°C to yield a 3.5% w/w solution. The solutions were filtered, allowed to cool at 5°C hr^{-1} to 15°C, and held at this temperature for 3 days. Theophylline monohydrate crystallized from the solution. The crystals were stored in a chamber maintained at 58% RH (saturated NaBr solution) at room temperature for 24 h. The chamber was fitted with an air-circulating fan that facilitated rapid attainment of equilibrium. Theophylline monohydrate crystals were milled with an agate mortar-pestle for ~5 min, and then in a ball-mill for 45 s. The milled material was sieved, and only particles ranging in size from 20 to 45 μm were used in the experiments. The powders were stored at 58% RH (room temperature) until used.

Preparation of Theophylline Monohydrate in Presence of PVP

The general procedure was the same as above, except that PVP (BASF Corporation, Germany) was dissolved in the recrystallization solutions. The grades of PVP used were K-12, K-25, K-90, which had an average molecular weight of ~10,000, 30,000 and 1,000,000, respectively. The concentration of PVP in the aqueous recrystallization solutions were 5, 10 and 15% w/w. The amount of PVP incorporated in the product crystals of theophylline monohydrate was determined by a modified colorimetric method (29–31). The presence of theophylline (theophylline to PVP weight ratios up to 100:1 w/w) did not have an effect on the quantification of PVP.

Physical Characterization

Differential Scanning Calorimetry (DSC)

A differential scanning calorimeter (Model 2920, TA Instruments, New Castle, DE) with a refrigerated cooling accessory was used. The instrument was calibrated with pure samples of tin and indium. About 4–5 mg sample was packed in aluminum pans, crimped with lids having several pinholes, and heated under dry nitrogen purge (70 ml/min) from 10 to 320°C.

Thermogravimetric analysis (TGA)

The sample was heated in an open aluminum pan from room temperature to 300°C, under nitrogen purge (70 ml/min), at 10°C/min in a thermogravimetric analyzer (Q50, TA Instruments). For isothermal studies, the sample was first heated at 20°C/min to the desired temperature (in the range of 40 to 65°C), and the weight loss was monitored as a function of time.

Powder X-ray diffractometry (XRD)

The sample was filled in an aluminum holder by the side-drift method, and was exposed to CuKα radiation (45 kV × 40 mA) in a wide-angle X-ray powder diffractometer (Model D5005, Siemens). The instrument was operated in a step scan mode and in increments of 0.01°2θ. The angular range was 5 to 40°2θ, and counts were accumulated for 1 s at each step.

Other Characterization Techniques

The theophylline monohydrate crystals were examined using an environmental scanning electron microscope. The monohydrate crystals were also subjected to hot stage microscopy. Finally, the diffuse reflectance spectra of the samples under dry air were recorded in a FTIR spectrophotometer.

Time Resolved Powder X-ray Diffractometry

Transmission geometry-sample preparation

In XRD employing transmission geometry, the incident X-ray beam passes through the sample and the diffraction pattern is acquired using a 2-dimensional area detector positioned on the opposite side of the sample (in relation to the X-ray source) (32,33). The vertical configuration of powder samples was made possible by filling the samples (~14 mg) in aluminum pans (used generally for differential scanning calorimetry, TA Instruments), and the pans were crimped non-hermetically. A special punch was designed to make uniformly spaced pin-holes on the pans and lids prior to filling the sample. This design was necessary to allow the water to escape following dehydration of the sample during the experiment. The sample preparation (weighing, filling and crimping) was performed at room temperature in a glove box maintained at ~50% RH using humidified air.

Synchrotron beamline

Experiments were performed on the ID2 beamline at the European Synchrotron Radiation Facility (ESRF). The beamline, equipped with an undulator, provided a highly collimated and intense X-ray beam. A 2-dimensional charge coupled device detector (Photonic Science Ltd., UK) was used for acquiring the diffraction data. Diffraction patterns were recorded in transmission mode, with exposure time of 40 ms. The signal-to-noise ratio was improved by integrating successive frames together, and the number of frames depended on the time taken to complete the experiment. During each experiment, 144 to 248 diffraction patterns (frames) could be recorded continuously with no dead time between frames. Calibration was performed using an Al_2O_3 standard (SRM 764a, NIST). The specific details of the X-ray beam characteristics, the sample chamber, and the data acquisition technique have been described earlier (33).

The sample (~14 mg), filled in a crimped (DSC) pan, was placed vertically on the sample stage arm (maintained at RT). The main sample chamber was pre-heated to the desired temperature. On activation of an electronic trigger, the sample stage arm moves very rapidly into the pre-heated sample chamber, thus exposing the sample to the incident X-ray beam. Simultaneously, the trigger signal activates the data acquisition system. Diffraction data were obtained continuously as snapshots with time resolution of 40 ms, in the transmission geometry, as the sample was held under isothermal conditions. The integration time for each successive powder diffraction pattern was adjusted between 0.5 and 10 s. The dehydration of theophylline monohydrate (**M**) was studied isothermally at several temperatures in the range of 60 to 130°C. At the end of each experiment, the sample chamber was heated to 150°C to allow complete conversion of the sample to the stable anhydrate (**A**).

Experiments on a Rotating Anode X-ray Diffractometer

A rotating anode (Rigaku, RU-200BVH) X-ray generator was used to obtain X-rays. The XRD instrument, equipped with Franks focusing optics, was set-up for diffraction measurements in the transmission geometry. The operating power of the X-ray generator was 2.5 to 8 kW. The two dimensional diffraction patterns were collected using a multiwire area detector (HISTAR®, Bruker, WI). Software routines were developed for acquiring X-ray diffraction patterns continuously (minimal dead time between successive frames) with a 10–30 s integration time per pattern.

The sample (~14 mg), filled in a crimped DSC pan, was placed on the sample stage and a powder pattern was recorded at room temperature. The sample was then removed from the stage, the stage heated to the desired temperature, and the sample reinserted into the chamber. The dehydration of **M** was studied isothermally at several temperatures in the range of 35 to 80°C. At the end of each experiment, the sample chamber was heated to 150°C to allow complete conversion of the sample to the stable anhydrate (**A**). Diffraction data were obtained continuously with time resolution of 10–30 s per pattern.

RESULTS AND DISCUSSION

Physical Characterization

X-ray Diffractometry

The powder XRD pattern of theophylline monohydrate recrystallized from water and PVP solutions was in agreement with the pattern reported in the Powder Diffraction File maintained by the International Centre for Diffraction Data (34). The powder patterns of **M**, **A*** and **A** show pronounced differences (Fig. 1). The peaks unique to each

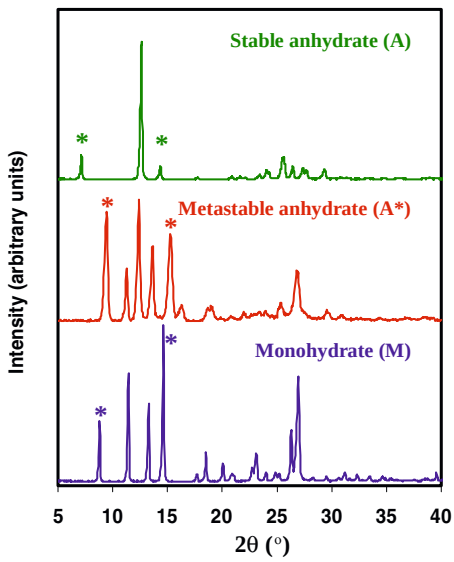

Fig. 1. Powder X-ray diffraction patterns of theophylline phases. The peaks unique to each phase are marked by *asterisks*.

Table I. Comparison of FWHM (full width at half maximum) Values of X-ray Peaks of Milled and Unmilled Theophylline Monohydrate Samples

Peak Position (°2θ)	Milling Time (min)	Full Width at Half Maximum (FWHM, °2θ)			
		I	II	III	Mean
8.84	0	0.16	0.15	0.15	0.15 (±0.01)
	4	0.14	0.16	0.17	0.16 (±0.01)
	10	0.17	0.14	0.14	0.15 (±0.01)
11.47	0	0.17	0.15	0.15	0.16 (±0.01)
	4	0.15	0.17	0.18	0.16 (±0.01)
	10	0.17	0.15	0.15	0.16 (±0.01)

phase (for example, **M**, **A***, and **A** show characteristic peaks at 7.2, 8.4 and 9.4°2θ, respectively), can be used for phase identification and quantification. The effect of grinding on the crystallinity of theophylline monohydrate was ascertained by comparing the width of the X-ray peaks (measured as full width at half maximum, FWHM) for samples milled for various time periods (0 to 8 min). A decrease in crystallinity will result in a decrease in peak height accompanied by an increase in FWHM. The similar FWHM values (Table I) indicate that milling of theophylline monohydrate did not alter the crystallinity of the material.

Microscopy

The environmental scanning electron micrographs revealed that the theophylline monohydrate samples did not possess a pronounced habit and that the particles were essentially <45 μm in size. The morphology of the crystals obtained in the presence and absence of PVP were similar.

Thermal Analysis

Non-isothermal TGA of theophylline monohydrate revealed a weight loss of 8.9% in the temperature range of 25 to 110°C, equivalent to the stoichiometric water content in theophylline monohydrate (Fig. 2). The weight loss occurred in two steps, suggesting biphasic water removal from theophylline monohydrate. The corresponding DSC curves of **M** also indicated broad overlapping dehydration endotherms in the temperature range of 25 to 90°C (Fig. 2). An endotherm seen at 174°C was attributed to melting of anhydrous theophylline formed on dehydration (not shown).

Interestingly, the isothermal TGA curves also revealed a biphasic weight loss (Fig. 3). The experiments were performed

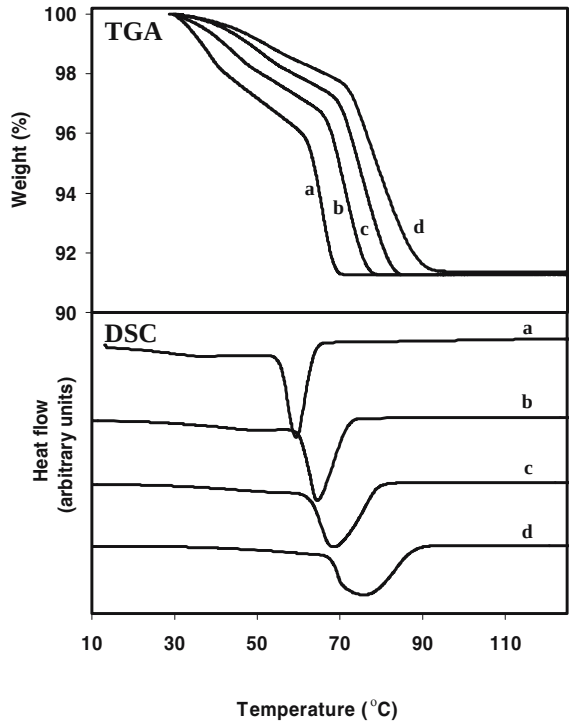

Fig. 2. DSC and TGA curves of theophylline monohydrate at different heating rates: (a) 2°C/min; (b) 5°C/min; (c) 10°C/min; and (d) 20°C/min.

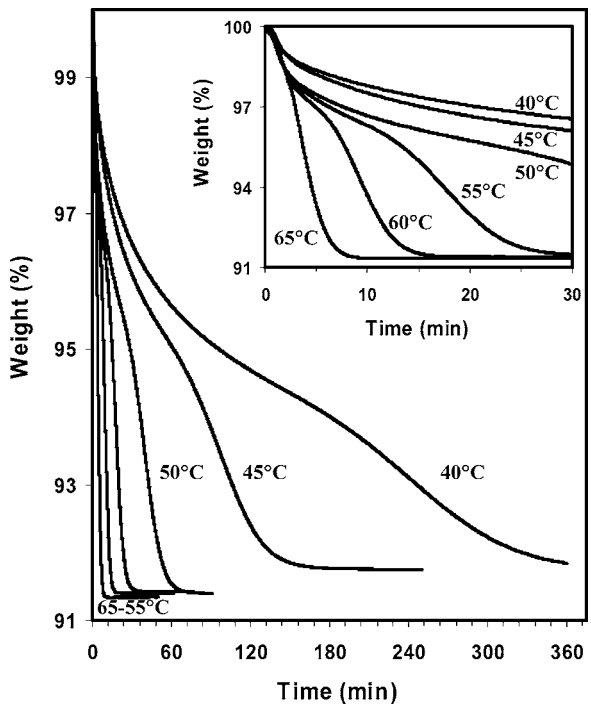

Fig. 3. Isothermal TGA of theophylline monohydrate at different temperatures. The inset is an expanded TGA profile showing data up to 30 min.

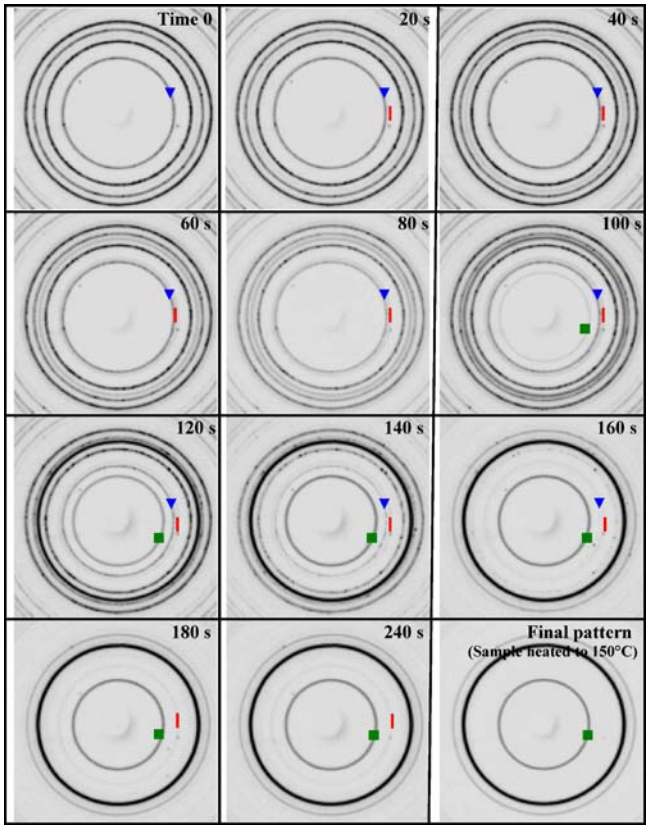

Fig. 4. Two-dimensional powder XRD patterns acquired during isothermal dehydration of theophylline monohydrate at 80°C. The characteristic Debye rings of the monohydrate (▾), anhydrous metastable (▮), and anhydrous stable (■) forms of theophylline have been indicated. The reaction was carried out for 300 s, after which the sample was heated to 150°C.

in the temperature range of 40 to 65°C. The complex weight loss profiles obtained in the isothermal studies indicate that there may be change in the reaction mechanism during the course of the reaction. Thus, the two-step process indicated in the non-isothermal DSC and TGA may not be entirely due to simple dehydration and vaporization of water during **M→A** transformation. This conclusion was further supported by the identification of both $\mathbf{A}^*$ and **A** in the dehydrated samples by XRD (results not shown). Careful observation of the TGA curves reported by Agbada and York also indicate a complex dehydration profile, especially at lower dehydration temperatures (≤70°C) (4). However, as noted earlier, these authors assumed a single **M→A** transition. Duddu *et al*. investigated the dehydration reaction using isothermal microcalorimetry (10). Based on the deconvolution of the power-time data from the thermal activity monitor, they proposed a two-step dehydration process at 40°C.

The main limitation of the thermoanalytical techniques is that they do not provide information on the individual phases present during a reaction. Powder XRD, on the other hand, allows unambiguous identification of the crystalline phases present in a system. Simultaneous quantification of multiple crystalline phases is possible because each phase is usually characterized by its unique X-ray pattern. Therefore, our next objective was to utilize time-resolved XRD to investigate the dehydration reaction in detail.

Two-Dimensional XRD for Study of Rapid Solid State Reactions

The limitation often encountered when using conventional XRD is in time resolution and sensitivity. Thus although XRD can provide direct information on the changes occurring in the crystal lattice of a material, in several cases, the time for acquiring diffraction patterns is greater than the time course of the solid state reaction. These limitations can be overcome with the use of high intensity radiation and rapid data collection, using a 2-dimensional detector (33). The dehydration of theophylline monohydrate was investigated using a high intensity beamline at the European Synchrotron Radiation Facility. A representative set of 2-dimensional powder diffraction patterns collected during isothermal dehydration of theophylline monohydrate at 80°C is shown (Fig. 4). As dehydration occurs, a decrease in the intensity of the Debye rings due to theophylline monohydrate (**M**), and the appearance of rings due to the stable anhydrate phase (**A**) are observed. The powder patterns also reveal the transient existence of an intermediate phase. The d-spacings of this phase correspond to the metastable anhydrate ($\mathbf{A}^*$) previously reported by Phadnis and Suryanarayanan (12). Interestingly, it is seen

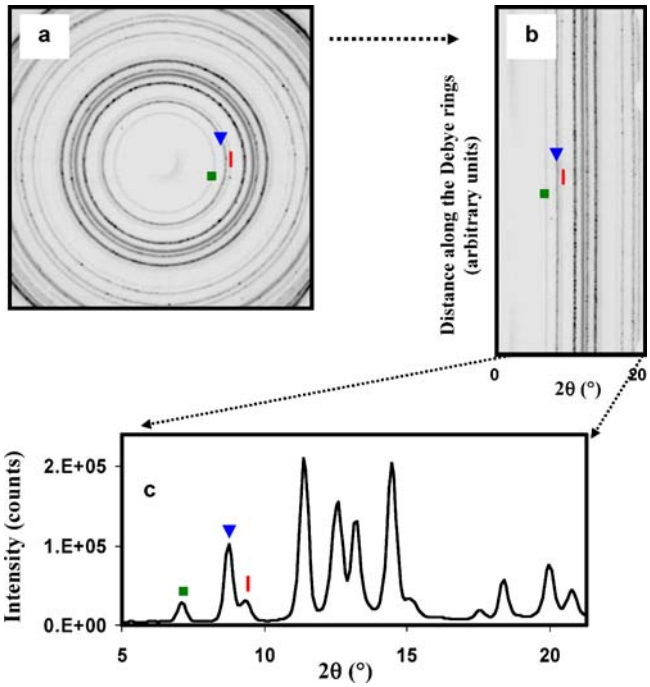

Fig. 5. Schematic representation of the conversion of a 2-dimensional X-ray patterns to 'intensity *versus* °2θ' format. (a) X-ray pattern of a powder sample containing the monohydrate (▾), anhydrous metastable (▮), and anhydrous stable (■) forms of theophylline. (b) Transformation of diffraction data from the Cartesian to polar coordinate system. The *x*-axis of the pattern is calibrated to indicate the position of the Bragg reflections (in °2θ). (c) 'Intensity *versus* °2θ' plot obtained by integration of intensities along each °2θ position in plot (b). The characteristic Bragg reflections for theophylline phases have been indicated.

that only **A*** is formed at the early stages of the dehydration reaction. It is noteworthy that even when the reaction is complete in less than 60 s, as in the case at 130°C, 120 powder diffraction patterns could be obtained (data not shown). In a conventional X-ray diffractometer, the acquisition of a single X-ray pattern typically requires 3 to 5 min. Another unique feature of 2-D XRD is that the powder patterns are obtained as a 'snapshot,' allowing simultaneous monitoring of the reactant (**M**), intermediate (**A***), and product (**A**) phases.

Each 2-dimensional X-ray pattern acquired during the dehydration reaction can be opened up by converting the intensity data from the Cartesian to the polar coordinate system (Fig. 5a and b). The intensities along the *y*-axis of the transformed pattern can be integrated at each °2θ position to obtain a plot of 'intensity *versus* °2θ' (Fig. 5c). Since the entire 2-dimensional data are utilized in the process, the effects due to preferred orientation are minimized.

An effective method to portray the large number of successive diffraction patterns collected during the 'time resolved' XRD experiments is via 3-dimensional plots or contour plots. The procedure is illustrated in Fig. 6. The successive 'intensity *versus* 2θ' patterns (each obtained from a 2-D diffraction pattern as described in the preceding paragraph) can be arranged as a sequence to obtain a 3-D plot, on which the *x*-axis represents '°2θ,' the *y*-axis denotes the 'time,' and the *z*-axis represents the 'intensity' (Fig. 6a). The 3-D plot can be visualized from the top (along the *z*-axis direction) to yield a contour plot. The diffracted intensity represented along the *z*-direction in a 3-D plot is rendered as a 'color shade' in a contour plot (Fig. 6b).

The contour plots comprehensively depict the changes occurring in the crystal lattice of a material during a solid state reaction (Fig. 7a). Extraction of the diffracted intensities along the *x*-axis (°2θ) at any fixed time allows identification and quantification of the crystalline phases present at that specific time period (Fig. 7b). On the other hand, measuring the change in the diffracted intensities as a function of time (i.e., along the *y*-axis) at a fixed 2θ value provides kinetic information pertaining to the appearance or disappearance of the corresponding crystalline phase (Fig. 7c).

In addition to the isothermal dehydration studies carried out at 130°C (Fig. 6), experiments were also conducted at 60, 80 and 110°C (results not shown). At high temperatures (130° and 110°C), **A*** had only a transient existence. The appearance of **A*** preceded the formation of **A**. The next step was to study the kinetics of the reactions so as to obtain a mechanistic understanding of the process. Due to limited beam time on the synchrotron source, systematic kinetic studies were performed on a diffractometer equipped with a rotating anode X-ray generator, focusing optics and a 2-dimensional area detector. Using this setup, the X-ray patterns could be obtained with a time resolution of 10 to 30 s.

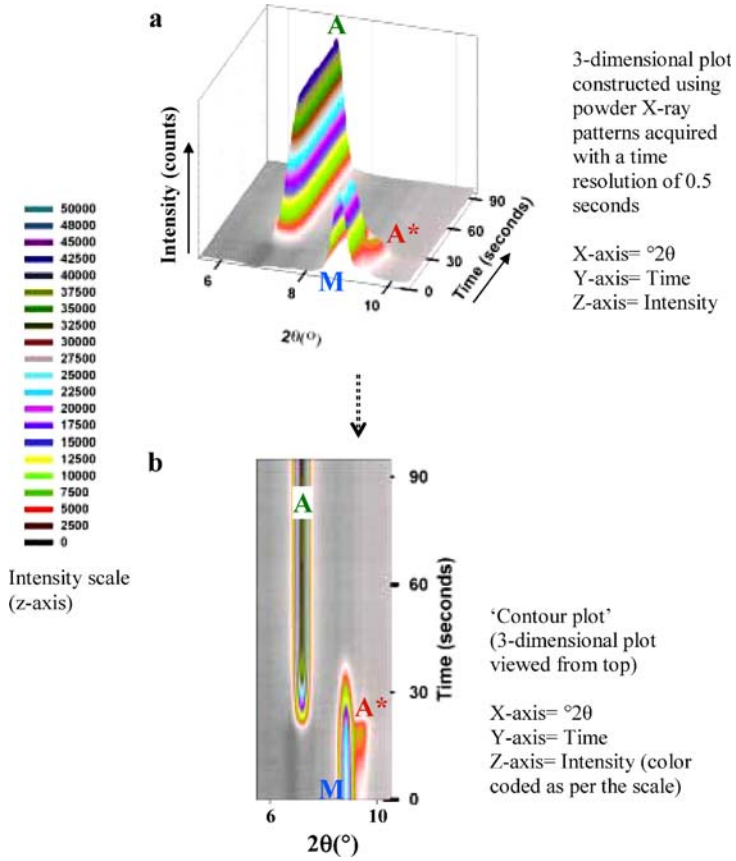

Fig. 6. Representation of successive X-ray patterns obtained during dehydration of theophylline monohydrate at 130°C as a 'contour plot.' The characteristic peaks of theophylline monohydrate (**M**), metastable anhydrate (**A***) and stable anhydrate (**A**) have been indicated.

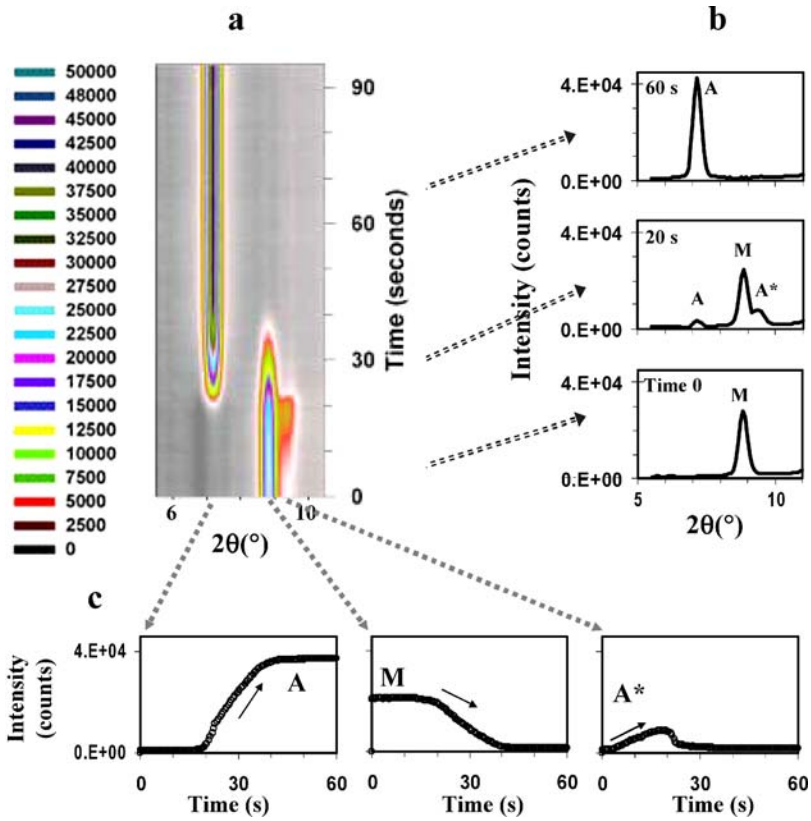

Fig. 7. (a) Contour plot showing dehydration of theophylline at 130°C. (b) Measurement of intensity data along the *x*-axis (°2θ) at fixed time points yields information on crystalline phases present during the reaction. (c) Kinetics of the disappearance and /or formation of theophylline monohydrate (**M**), metastable anhydrate (**A***), and stable anhydrate (**A**) monitored by measuring intensities of characteristic peaks as a function of time.

Dehydration Kinetics

Theoretical Basis for Quantitative Analysis Using XRD

The intensities of peaks unique to the crystalline reactant (**M**), intermediate (**A***) and product (**A**) phases can be used for quantification of each of these phases during the course of the reaction. The theoretical basis of the quantitative analysis of powder mixtures has been developed by Klug and Alexander (22,23). A solid mixture consisting of several phases can be regarded as consisting of only two components: the analyte (component '*J*'), and the sum of the other components designated as the matrix (component '*M*'). The relationship between peak intensity and the analyte weight fraction (x_J) in a powder mixture is given by:

$$\frac{(I_{iJ})}{(I_{iJ})_0} = x_J \qquad (1)$$

where, (I_{iJ}) is the intensity of line *i* of component *J* in a powder mixture and $(I_{iJ})_0$, is the intensity of the same line in a sample consisting only of *J*. The mass attenuation coefficients of theophylline monohydrate (μ^*_{mono}), and anhydrous theophylline (μ^*_{anhy}), were 6.89 and 6.55 cm^2g^{-1}, respectively (CuKα radiation). Because $\mu^*_{mono} \cong \mu^*_{anhy}$, the individual phases during the dehydration reaction can be quantified using Eq. (1).

Although the powder patterns of **M**, **A*** and **A** are different, there was a significant overlap of the diffraction peaks (Figs. 1 and 5) which posed a challenge in accurate extraction of peak intensity values for individual phases. It is recognized that the integrated intensity is a more reliable measure than peak intensity (height). Thus for obtaining quantitative information on the composition of the sample, the overlapping peaks were resolved. Profile shape functions (PSF) were used to model the overlapped peaks (32). Once the individual peaks were resolved, the values of integrated intensities of the characteristic peaks for **M**, **A*** and **A** were employed for quantitative analysis.

Dehydration Pathway and Kinetics of Theophylline Monohydrate

The dehydration reaction of theophylline monohydrate was studied isothermally at several temperatures in the range of 35 to 80°C. The unique peaks of **M**, **A*** and **A** at 7.2, 8.4 and 9.4°2θ, respectively, were separated via the profile fitting approach. The weight fractions of the reactant (**M**), intermediate (**A***), and the product (**A**) phases could thus be determined as a function of time.

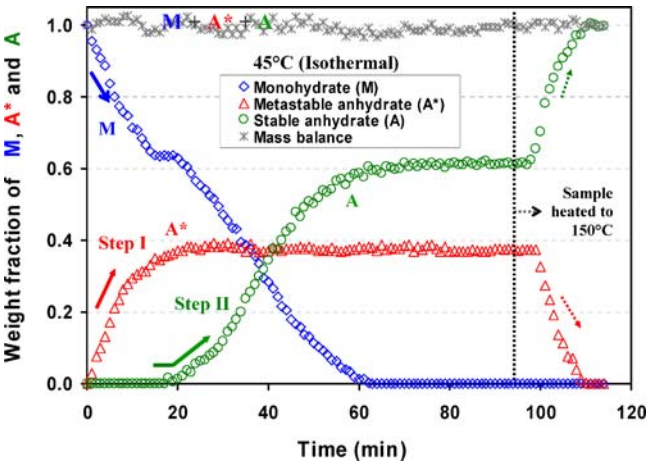

Fig. 8. Dehydration kinetics of theophylline monohydrate at 45°C. The disappearance of **M** is accompanied by a two stage appearance of the theophylline anhydrous polymorphs (**A*** and **A**).

A representative kinetic profile of individual theophylline phases during isothermal dehydration at 45°C is shown (Fig. 8). During the isothermal dehydration process, the concentration of **M** in the sample continued to decrease. Interestingly, the kinetic profile for the disappearance of **M** showed a 'kink.' Our attempts to fit the dehydration data to any of the commonly used solid state models were unsuccessful (35,36). It is noteworthy that in the early stages of the reaction, the disappearance of **M** is accompanied by the formation of only the metastable anhydrate (**A***). Thus, the reaction in the early stages can be represented as **M**→**A*** (Step I in Scheme 1). There was a lag time associated with the formation of **A**. Interestingly, once the stable polymorph (**A**) appears, the concentration of the metastable polymorph (**A***) reaches a plateau. Thus the kinetic data strongly suggest that once the stable polymorph appears, the remainder of reaction proceeds by the **M**→**A** pathway (Step II in Scheme 1). At the end of the dehydration reaction, i.e., when **M** is completely depleted, both the **A*** and **A** exist in the dehydrated product. The **A***→**A** conversion is comparatively slow. On heating the sample to 150°C, there is complete conversion of **A***→**A**. Phadnis and Suryanarayanan have indicated that though the **A***→**A** conversion is slow at room temperature, the rate of conversion is accelerated in presence of water vapor (12). Thus, depending on the storage conditions, the conversion of **A***→**A** may occur over a period of few days or may take several months. The *in situ* conversion of **A***→**A** can have adverse effect on the product performance and hence the concentration of **A*** in a drug product must be controlled.

Based on the evaluation of the kinetic profiles of **M**, **A*** and **A**, we propose the following reaction model.

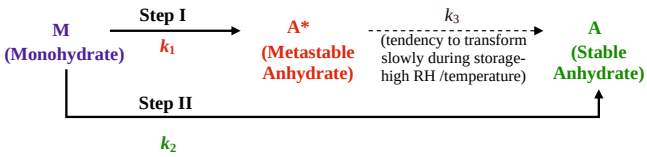

Scheme 1. Dehydration pathway of theophylline monohydrate.

The kinetics of the appearance of metastable anhydrate (**A***, step I in the above scheme) was best described by a first-order rate equation (Fig. 9).

$$[A_1] = [A_1]_\infty \left(1 - e^{-k_1 t}\right) \tag{2}$$

where, $[A_1]$ is the weight fraction of product (in this case **A***) at time t, $[A_1]_\infty$ is the fraction at the end of the dehydration reaction, and k_1 is the corresponding rate constant. The model selection was based on the value of coefficient of correlation, r, obtained after fitting the data to common solid-state reaction models (35,36).

Similarly the rate of appearance of the stable anhydrous polymorph (**A**) was best described by the Avrami-Erofeev 3-dimensional nucleation and growth model (Fig. 9).

$$[A_2] = [A_2]_\infty \left(1 - e^{-(k_2(t-t_0))^3}\right) \tag{3}$$

where, $[A_2]$ is the weight fraction of product **A** at time t, $[A_2]_\infty$ is the weight fraction at the end of the dehydration reaction, t_0 is the lag time, and k_2 is the corresponding rate constant. The rate constant k_3 associated with the **A***→**A** conversion (Scheme 1) can be determined after **M** has been depleted (i.e., after **M**→**A*** and **M**→**A** pathways ceases to be active). It was observed though that the rate of conversion was very slow compared to the rates of the preceding reaction steps. Since the fraction converted was small, fitting

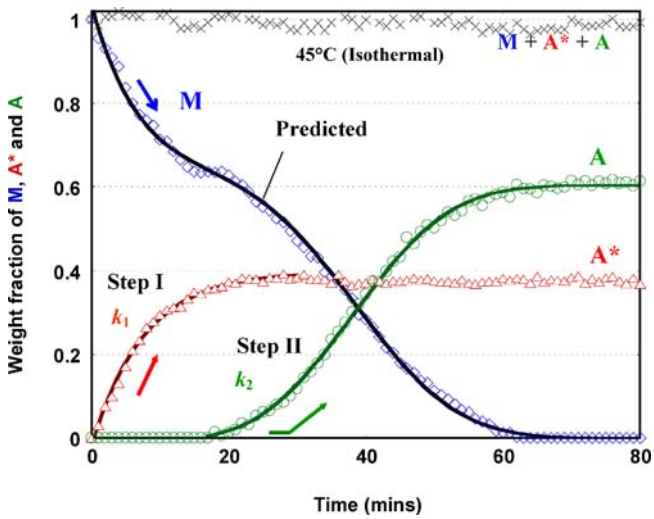

Fig. 9. Kinetics of the disappearance of theophylline monohydrate (**M**), and the two step appearance of anhydrous theophylline polymorphs (**A*** and **A**). Experimental data for appearance of **A*** and **A** were modeled (superimposed solid lines) using Avrami-Erofeev equations with exponents 1 (first order) and 3 (3-dimensional growth of nuclei), respectively. The *black solid line* (labeled as 'predicted') is the simulated kinetic profile for disappearance of **M** obtained using the model proposed for the dehydration reaction pathway (Scheme 1).

Table II. Rate Constants Determined for Dehydration of Theophylline Monohydrate at 45°C, According to Scheme 1

	Parameter	Value	SD	CV	95% Confidence Interval	
Simultaneous modeling of kinetic data	k_1 (min^{-1})	1.40×10^{-1}	3.35×10^{-3}	2.39×10^{0}	1.34×10^{-1}	1.47×10^{-1}
	k_2 (min^{-1})	2.96×10^{-2}	2.24×10^{-4}	7.57×10^{-1}	2.92×10^{-2}	3.01×10^{-2}
	t_0 (min, step II)	9.21×10^{-0}	2.26×10^{-1}	2.46×10^{0}	8.77×100	9.66×10^{0}
	k_3 (min^{-1})	1.15×10^{-4}	8.83×10^{-5}	7.69×10^{1}	5.99×10^{-5}	2.89×10^{-4}
Modeling of kinetic data as individual reaction steps	k_1 (min^{-1})	1.40×10^{-1}	3.37×10^{-3}	2.41×10^{0}	1.34×10^{-1}	1.47×10^{-1}
	k_2 (min^{-1})	2.97×10^{-2}	8.13×10^{-4}	2.74×10^{0}	2.81×10^{-2}	3.13×10^{-2}
	t_0 (min, step II)	9.20×10^{0}	3.62×10^{-1}	3.93×10^{0}	8.48×10^{0}	9.91×10^{0}
	$k_3 \cong 0$ during the time frame of the experiment					

of the experimental data to reaction models, and obtaining reliable estimate of the rate constant k_3 was not feasible ($k_3 \cong 0$ during the experimental time frame). As mentioned earlier, the **A***→**A** conversion may occur over a period of several months (12).

To ascertain the validity of the two-step reaction model (Scheme 1), the rate of disappearance of **M** was simulated using the parameters obtained from Eqs. (2) and (3). The overlay of the simulated curve and the experimental data for the disappearance of **M** is shown in Fig. 9. There is a good agreement between the simulated curve and experimental data, and the two-stage ('kink') disappearance of **M** may be explained by the proposed reaction scheme. The kinetic data for **M**, **A*** and **A** were also analyzed using the SAAM II software (numerical module, SAAM Institute Inc. WA). The rate constants were determined numerically by simultaneous modeling of the kinetic data. The rate constants determined by simultaneous modeling (**M**→**A***; **M**→**A**; **A***→**A**) were similar to those obtained by fitting of the individual reaction steps (Table II).

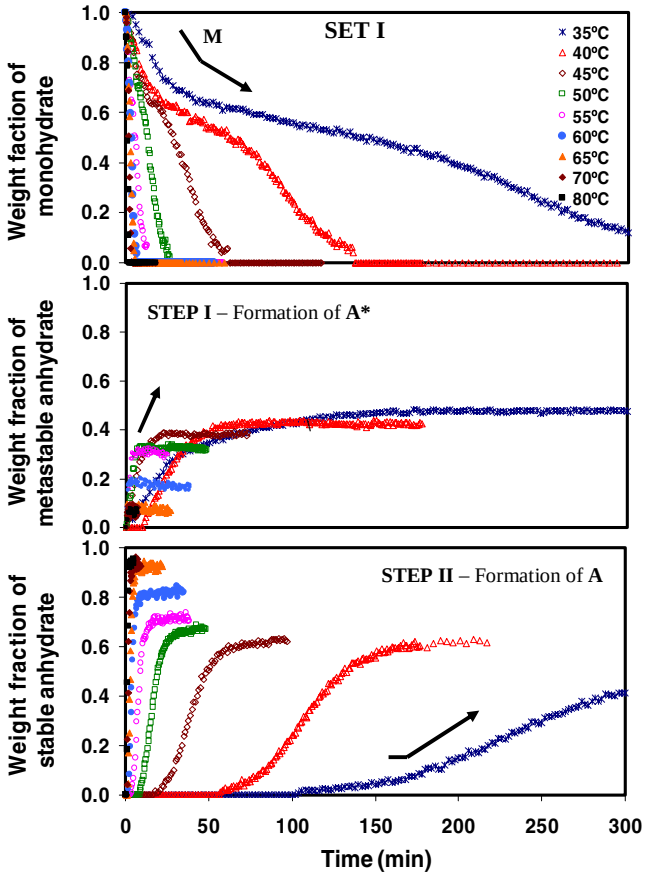

Fig. 10. Isothermal dehydration kinetics of theophylline monohydrate (data set I). The kinetic plots indicate a two-step dehydration process.

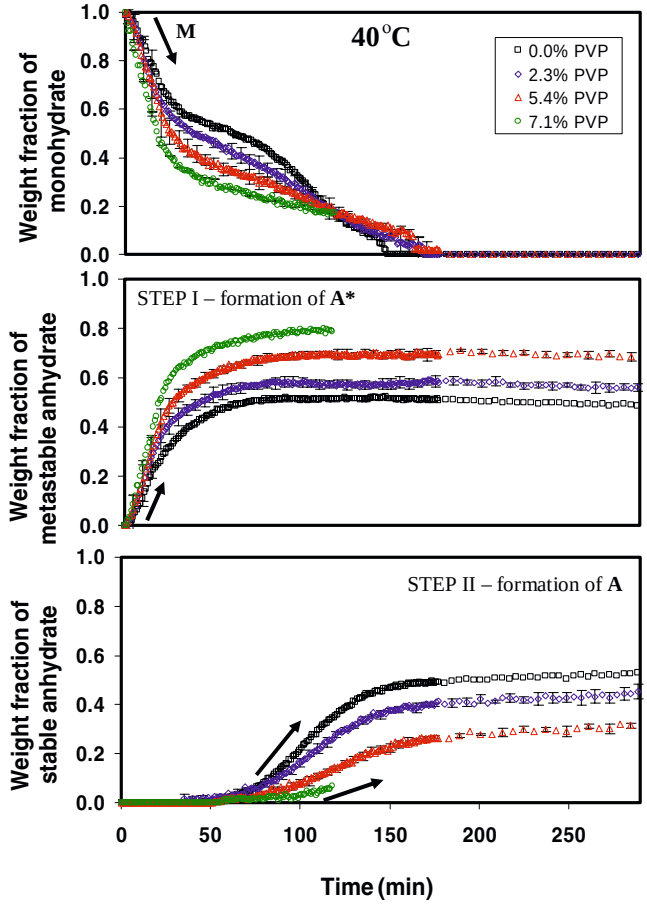

Fig. 11. Effect of PVP on the theophylline monohydrate dehydration (40°C) reaction kinetics and pathway. *Error bars* indicate SD ($n = 3$).

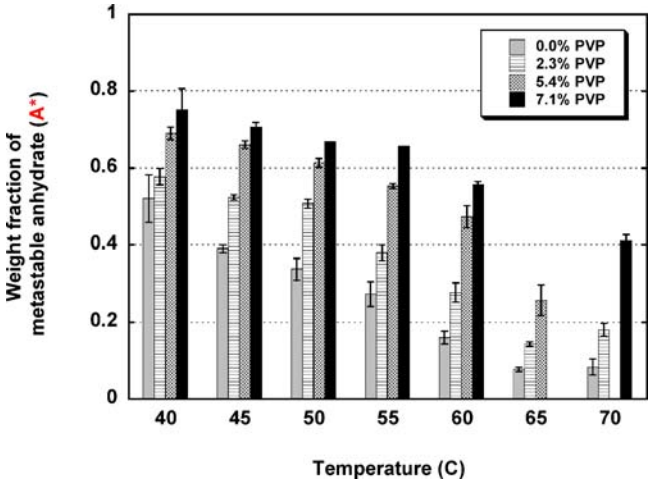

Fig. 12. Effect of PVP on the amount of metastable anhydrate in the product phase obtained following the dehydration of theophylline monohydrate. *Error bars* indicate SD (n = 3).

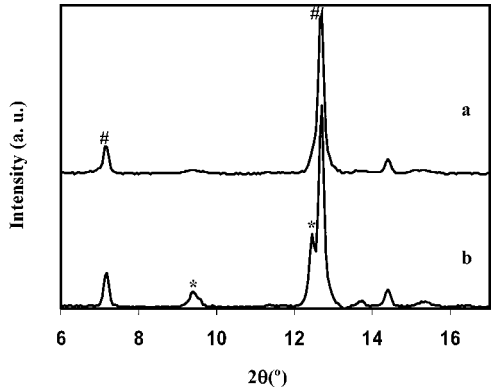

Fig. 13. Powder X-ray patterns of theophylline monohydrate crystals dehydrated at 40°C. (**a**) Samples obtained from the region near the center of the crystals. (**b**) Samples obtained form the region near the ends of the crystals. The peaks characteristic to the stable anhydrate (#) and metastable anhydrate (*) are indicated.

The two-stage water loss from theophylline monohydrate was observed at isothermal dehydration temperatures in the range of 35 to 80°C. One representative kinetic profile is shown (Fig. 10). At each temperature, the reaction was studied in triplicate. The metastable anhydrous polymorph (**A***) and the stable polymorph (**A**) are the reaction products in step I and in step II, respectively. The relative content of **A*** and **A** in the anhydrous product phase is dependent on the dehydration temperature. There is an increased build-up of metastable anhydrate at low dehydration temperatures (summarized later in Fig. 12).

Effect of PVP on the Dehydration Kinetics of Theophylline Monohydrate

The dehydration kinetics of **M**, in presence of different concentrations of PVP, was evaluated at several temperatures. Let us consider the dehydration kinetics at 40°C as a representative case (Fig. 11). Comparison of the kinetic curves of **M**, **A*** and **A** indicate that the water loss is a two-step process even in the presence of PVP. The **A*** is formed in the early stage of the reaction, whereas **A** is formed at a later stage. Interestingly, PVP has a pronounced inhibitory effect on the rate of the formation of stable anhydrate (i.e., **M**→**A**, step II). The rate of formation of **A*** (i.e., **M**→**A***, step I) shows a slight increase. Thus the effect of PVP on the reaction pathway can be schematically represented as follows. (Scheme 2)

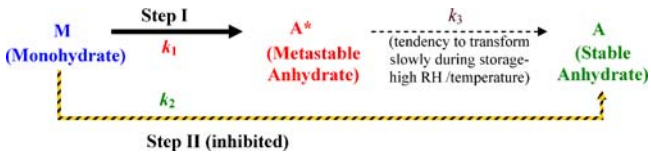

Scheme 2. Effect of PVP on the dehydration kinetics of theophylline monohydrate.

Because the **M**→**A*** reaction precedes the **M**→**A** reaction, inhibition of the latter step led to a build-up of **A*** in the dehydrated product. The inhibitory effect of PVP on the formation of the stable anhydrate (**A**) was proportional to the PVP concentration in the sample. Similar systematic effect of PVP on the build-up of **A*** was seen at several other temperatures (40 to 70°C). As in the case with samples containing no PVP, the relative content of the two anhydrous polymorphs (**A*** and **A**) in the dehydrated product was also dependent on the temperature of dehydration. Thus, there was an increased build-up of metastable anhydrate (i) at low dehydration temperatures and (ii) at high PVP concentration (Fig. 12).

Loss of Water from Theophylline Monohydrate Crystals

Lin and Byrn have described the dehydration process of theophylline monohydrate using hot stage microscopy (at 35°C) (5). The dehydration was initiated at the ends of the crystals and proceeded towards the center. Interestingly, in the later stages of the reaction, desolvation occurred from the sides of the crystal. Suzuki *et al.* also reported the sporadic appearance and growth of the nuclei of anhydrous theophylline on the surface of the monohydrate crystal at 48°C (37). Similar dehydration behavior was seen when needle shaped theophylline monohydrate crystals were dehydrated at 40°C. Video enhanced microscopy revealed that dehydration was initiated at the ends of the crystals (results not shown). After a lag time, sporadic growth of nuclei was observed at the surface of the crystals (accompanied by formation of cracks on the surface). Each dehydrated crystal was cleaved into two zones: zone 1 corresponding to the two ends and zone 2 corresponding to the central region. Powder XRD, was performed on samples from these two zones (Fig. 13). Metastable anhydrate (**A***) was readily detected in zone 1. Thus, the microscopic observations and the XRD based kinetic studies indicate that the removal of lattice water at the early stages of dehydration may be responsible for the formation of the **A*** (for instance, at the ends of the crystals). The formation of the A is a nucleation controlled event (probably at the sur-

face of the crystals) which occurs at a later stage of the dehydration reaction. Once the stable polymorph appears, the dehydration predominantly occurs via the **M→A** pathway.

Effect of PVP on the Crystallization of Stable Anhydrate

There is recognition in the literature that reactions in crystalline solids usually begin at sites of crystal defects (38–44). Nucleation initiates at the high energy sites because the activation energy for reaction at these disordered regions is less than that at the perfect lattice sites. Once the product is formed, it becomes a source of strain in the crystal lattice, and disrupts the molecular interactions of the neighboring molecules causing them to react. In the PVP-theophylline system, the PVP may accumulate near the grain boundaries of polycrystalline theophylline monohydrate. The kinetic modeling of the XRD data, as well as the microscopic observations suggest that the formation of **A** is likely to be nucleation controlled. If this is indeed the case, PVP may interfere with the nucleation and/or growth of the stable anhydrate during the dehydration reaction. In addition, there can also be a specific interaction, such as hydrogen bonding, between PVP and theophylline. PVP can act as a proton acceptor (via the *O* atom of the pyrrole ring) whereas, theophylline can act as a proton donor (aldimine group) (45–48). A change in the hydrogen bonding in theophylline should be reflected as changes in the *N–H* stretching vibration, whereas hydrogen bond formation between PVP and theophylline should be reflected by shift in the PVP carbonyl stretching vibration (45–47). Investigation of this aspect by FTIR was attempted, however the results obtained were inclusive (data not shown). The underlying causes could be low concentration and heterogeneous distribution of PVP, interference due to water or the weak nature of the interaction.

Pharmaceutical Significance

Previous studies have revealed that *in situ* $\mathbf{A}^*\rightarrow\mathbf{A}$ transition in theophylline tablets caused tablet hardening and dissolution failure (12). In order to avoid phase transition induced tablet hardening, it is necessary to control the physical form of theophylline during processing (specifically at the end of granulation process) and minimize the concentration of $\mathbf{A}^*$ in the granules. Interestingly, $\mathbf{A}^*$ is formed only by dehydration of **M**. Two-dimensional XRD revealed that the dehydration of **M** is a two step process, with the first and second steps leading to the formation of $\mathbf{A}^*$ and **A**, respectively. Since the formation of $\mathbf{A}^*$ precedes the formation of **A**, a decrease in the rate of formation of **A** will result in a build up of $\mathbf{A}^*$ in the dehydrated product. The inhibitory effect of excipients (such as PVP) can have a profound effect on the physical form of the API in the final product. Phadnis and Suryanarayanan have reported that $\mathbf{A}^*$ is probably related monotropically to **A** (12). If $\mathbf{A}^*$ is present in the final product, there is a potential risk of *in situ* phase conversion during storage. A mechanistic understanding of the dehydration reaction pathway can help in the development of appropriate formulation and processing strategies so as to limit the formation of $\mathbf{A}^*$ in a formulation. These may include careful selection of excipients, increasing the drying temperature of granules, and alternate tableting technologies (for e.g., roller compaction and direct compression).

CONCLUSIONS

An X-ray diffractometric method, with the capability to monitor very rapid solid state reactions, was developed. Two-dimensional powder diffraction patterns were acquired with a time resolution of 40 ms using synchrotron X-radiation. The effects due to preferred orientation were minimized by acquiring data over the entire Debye rings. The dehydration reaction of theophylline monohydrate (**M**) was investigated using the 2-D XRD technique. Kinetic modeling of the diffraction data revealed that the dehydration of **M** occurred through a multi-step pathway involving the formation of the metastable anhydrous ($\mathbf{A}^*$) polymorph. The dehydration was initiated with the $\mathbf{M}\rightarrow\mathbf{A}^*$ transition, followed by the **M→A** transition. Lower dehydration temperatures resulted in higher concentration of $\mathbf{A}^*$ in the dehydrated product. PVP retarded the formation of **A** resulting in a build-up of $\mathbf{A}^*$ in the dehydrated product.

ACKNOWLEDGMENTS

A part of this work was made possible by the allocation of beam time at the European Synchrotron Radiation Facility (ESRF), Grenoble, France. We thank Dr. Theyencheri Narayanan, Scientist in Charge, ID2 High Brilliance Beamline, ESRF for his assistance and support. The scientific and technical support provided by Dr. Ramprakash Govindarajan is gratefully acknowledged.

REFERENCES

1. D. J. Sutor. The structures of the pyrimidines and purines. VI. The crystal structure of theophylline. *Acta Crystallogr.* **11**:83–87 (1958).
2. C. Sun, D. Zhou, D. J. W. Grant, and V. G. Young Jr. Theophylline monohydrate. *Acta Crystallogr.* **E58**:368–370 (2002).
3. A. A. Naqvi and G. C. Bhattacharyya. Crystal data for anhydrous theophylline. *J. Appl. Crystallogr.* **14**:464 (1981).
4. C. Agbada and P. York. Dehydration of theophylline monohydrate powder: effects of particle size and sample weight. *Int. J. Pharm.* **106**:33–40 (1994).
5. C. T. Lin and S. R. Byrn. Desolvations of solvated organic crystals. *Molr. Cryst. Liq. Cryst.* **50**:99–104 (1979).
6. M. Otsuka, N. Kaneniwa, K. Kawakami, and O. Umezawa. Effect of surface characteristics of theophylline anhydrate powder on hygroscopic stability. *J. Pharm. Pharmacol.* **42**: 606–610 (1990).
7. M. Otsuka, N. Kaneniwa, K. Kawakami, and O. Umezawa. Effects of tableting pressure on hydration kinetics of theophylline anhydrate tablets. *J. Pharm. Pharmacol.* **43**:226–231 (1991).
8. E. Shefter, H.-L. Fung, and O. Mok. Dehydration of crystalline theophylline monohydrate and ampicillin trihydrate. *J. Pharm. Sci.* **62**:791–794 (1973).
9. E. Suihko, J. Ketolainen, A. Poso, M. Ahhlgren, J. Gynther, and P. Paronen. Dehydration of theophylline monohydrate—a two step process. *Int. J. Pharm.* **158**:47–55 (1997).
10. S. P. Duddu, N. G. Das, T. P. Kelly, and T. D. Sokoloski. Microcalorimetric investigation of phase transitions. I. Is water desorption from theophylline.HOH a single-step process? *Int. J. Pharm.* **114**:247–256 (1995).

11. M. T. Ledwidge and O. I. Corrigan. Effects of environmental factors on the dehydration of diclofenac HEP dihydrate and theophylline monohydrate. *Int. J. Pharm.* **147**:41–49 (1997).
12. N. V. Phadnis and R. Suryanarayanan. Polymorphism in anhydrous theophylline—implications for the dissolution rate of theophylline tablets. *J. Pharm. Sci.* **86**:1256–1263 (1997).
13. E. Suihko, V. P. Lehto, J. Ketolainen, E. Laine, and P. Paronen. Dynamic solid-state and tableting properties of four theophylline forms. *Int. J. Pharm.* **217**:225–236 (2001).
14. ICH (International Conference on Harmonisation) Draft guidance on Q6A specifications: test procedures and acceptance criteria for new drug substances and new drug products: chemical substances. *Federal Register* **65**(251):83041–83063 (2000).
15. Process analytical technology—a framework for innovative pharmaceutical manufacturing and quality assurance. Draft guidance. U.S. Department of Health and Human Services. Food and Drug Administration. *Federal Register* **68**(172):52781–52782 (2003).
16. K. R. Morris, U. J. Griesser, C. J. Eckhardt, and J. G. Stowell. Theoretical approaches to physical transformations of active pharmaceutical ingredients during manufacturing processes. *Adv. Drug Deliv. Rev.* **48**:91–114 (2001).
17. S. Byrn, R. Pfeiffer, M. Ganey, C. Hoiberg, and G. Poochikian. Pharmaceutical solids: a strategic approach to regulatory considerations. *Pharm. Res.* **12**:945–954 (1995).
18. S. R. Byrn, W. Xu, and A. W. Newman. Chemical reactivity in solid-state pharmaceuticals: formulation implications. *Adv. Drug Deliv. Rev.* **48**:115–136 (2001).
19. S. K. Rastogi, M. Zakrzewski, and R. Suryanarayanan. Investigation of solid-state reactions using variable temperature X-ray powder diffractometry. II. Aminophylline monohydrate. *Pharm. Res.* **19**:1265–1273 (2002).
20. D. Giron. Thermal analysis and calorimetric methods in the characterization of polymorphs and solvates. *Themochim. Acta* **348**:1–59 (1995).
21. D. Giron. Characterization of pharmaceuticals by thermal analysis. *Am. Pharm. Rev.***3**:53–54, 56, 58–61 (2000).
22. H. P. Klug and L. E. Alexander. *X-ray Diffraction Procedures for Polycrystalline and Amorphous Materials*, Wiley, New York, 1974.
23. R. Suryanarayanan. X-ray powder diffractometry. In H. G. Brittain (ed.), *Physical Characterization of Pharmaceutial Solids*, Marcel Dekker, New York, 1995, pp. 187–221.
24. M. Otsuka, N. Kaneniwa, K. Otsuka, K. Kawakami, and O. Umezawa. Effect of tableting pressure and geometrical factor of tablet on dehydration kinetics of theophylline monohydrate tablets. *Drug Dev. Ind. Pharm.* **19**:541–557 (1993).
25. M. Karjalainen, S. Airaksinen, J. Rantanen, J. Aaltonen, and J. Yliruusi. Characterization of polymorphic solid-state changes using variable temparature X-ray powder diffraction. *J. Pharm. Biomed. Anal.* **39**:27–32 (2005).
26. S. Airaksinen, M. Karjalainen, E. Rasanen, J. Rantanen, and J. Yliruusi. Comparison of the effects of two drying methods on polymorphism of theophylline. *Int. J. Pharm.* **276**:129–141 (2004).
27. J. Tank. *Changes in Solid-State of Theophylline upon Wet Granulation*, M.S. dissertation, Department of Pharmaceutics, University of Minnesota, 1997.
28. M. Yoshioka, B. C. Hancock, and G. Zografi. Inhibition of indomethacin crystallization in poly(vinylpyrrolidone) coprecipitates. *J. Pharm. Sci.* **84**:983–986 (1995).
29. R. L. Larkin and R. E. Kupel. Quantitative analysis of poly(vinylpyrrolidinone) atmosphere samples and biological tissues. *Am. Ind. Hyg. Assoc. J.* **26**:558–561 (1965).
30. G. B. Levy and D. Fergus. Microdetermination of polyvinylpyrrolidone in aqueous solution and in body fluids. *Anal. Chem.* **25**:1408–1410 (1953).
31. M. Savva, V. P. Torchilin, and L. Huang. Effect of polyvinylpyrrolidone on the thermal phase transition of 1,2-dipalmitoyl-*sn*-glycero-3-phosphocholine bilayer. *J. Colloid Interface Sci.* **217**:160–165 (1999).
32. C. Nunes. *Use of High-Intensity X-radiation in Solid-State Characterization of Pharmaceuticals*, Ph.D. dissertation, Department of Pharmaceutics, University of Minnesota, 2005.
33. C. Nunes, A. Mahendrasingam, and R. Suryanarayanan. Quantification of crystallinity in substantially amorphous materials by synchrotron X-ray powder diffractometry. *Pharm. Res.* **22**: 1942–1953 (2005).
34. Powder Diffraction File-2. *International Centre for Diffraction Data*. Newtown Square, Pennsylvania, 1996.
35. J. H. Sharp, G. W. Brindley, and B. N. N. Achar. Numerical data for some commonly used solid state reaction equations. *J. Am. Ceram. Soc.* **49**:379–382 (1966).
36. D. C. Monkhouse and L. Van Campen. Solid state reactions—theoretical and experimental aspects. *Drug Dev. Ind. Pharm.* **10**:1175–1276 (1984).
37. E. Suzuki, K. Shimomura, and K. Sekiguchi. Thermochemical study of theophylline and its hydrate. *Chem. Pharm. Bull.* **37**:493–497 (1989).
38. W. J. Dunning. Theory of crystal nucleation from vapour, liquid and solid systems. In W. E. Garner W. E. Garner (ed.), *Chemistry of the Solid State*, Academic, New York, 1955, pp. 159–183.
39. Y. V. Mnyukh. Molecular mechanism of polymorphic transitions. *Molr. Cryst. Liq. Cryst.* **52**:467–503 (1979).
40. Y. V. Mnyukh. Polymorphic transitions in crystals: Nucleation. *J. Cryst. Growth* **32**:371–377 (1976).
41. Y. V. Mnyukh and N. N. Petropavlov. Polymorphic transitions in molecular crystals. I. Orientations of lattices and interfaces. *J. Phys. Chem. Solids* **33**:2079–2087 (1972).
42. F. C. Tompkins. Decomposition reactions. In N. B. Hannay (ed.), *Reactivity of Solids*, Plenum, New York, 1976, pp. 193–232.
43. H. Schmalzried. Solid-state reactions. In N. B. Hannay N. B. Hannay (ed.), *Reactivity of Solids*, Plenum, New York, 1976, pp. 233–280.
44. A. K. Galwey. The reactivity of solids in thermal decomposition (crystolysis) reactions. In V. V. Boldyrev (ed.), *Reactivity of Solids: Past, Present and Future*, Blackwell Science, Malden, Massachusetts, 1996, pp. 15–42.
45. L. S. Taylor and G. Zografi. Spectroscopic characterization of interactions between PVP and indomethacin in amorphous molecular dispersions. *Pharm. Res.* **14**:1691–1698 (1997).
46. K. Khougaz and S.-D. Clas. Crystallization inhibition in solid dispersions of MK-0591 and poly(vinylpyrrolidone) polymers. *J. Pharm. Sci.* **89**:1325–1334 (2000).
47. T. Matsumoto and G. Zografi. Physical properties of solid molecular dispersions of indomethacin with poly(vinylpyrrolidone) and poly(vinylpyrrolidone-co-vinyl-acetate) in relation to indomethacin crystallization. *Pharm. Res.* **16**:1722–1728 (1999).
48. E. D. L. Smith, R. B. Hammond, M. J. Jones, K. J. Roberts, J. B. O. Mitchell, S. L. Price, R. K. Harris, D. C. Apperley, J. C. Cherryman, and R. Docherty. The determination of the crystal structure of anhydrous theophylline by X-ray powder diffraction with a systematic search algorithm, lattice energy calculations, and 13C and 15N solid-state NMR: a question of polymorphism in a given unit cell. *J. Phys. Chem. B.* **105**:5818–5826 (2001).